HHS Public Access

Author manuscript

Vet Comp Orthop Traumatol. Author manuscript; available in PMC 2023 May 24.

Published in final edited form as:

Vet Comp Orthop Traumatol. 2021 September ; 34(5): 327–337. doi:10.1055/s-0041-1730355.

Skeletal Manifestations of Heritable Disproportionate Dwarfism in Cats as Determined by Radiography and Magnetic Resonance Imaging

Lisa M. Anderson[1], **Derek B. Fox**[1], **Kari L. Chesney**[1], **Joan R. Coates**[1], **Bryan T. Torres**[1], **Leslie A. Lyons**[1]

[1]Department of Veterinary Medicine and Surgery, College of Veterinary Medicine, University of Missouri, Columbia, Missouri, United States

Abstract

Objective—The aim of this study was to characterize the radiographic alignment of thoracic and pelvic limbs and evaluate for intervertebral disc disease in cats with feline disproportionate dwarfism (FDD).

Study Design—Observational cross-sectional study. Radiographic joint orientation angles were measured in 10 thoracic and pelvic limbs from 5 FDD cats and compared with those angles measured in 24 thoracic limbs and 100 pelvic limbs from skeletally normal cats. Magnetic resonance imaging of the spine was performed in 2 FDD cats for the evaluation of pathology of the intervertebral discs or vertebrae.

Results—All limbs from FDD cats possessed deformities. FDD humeri demonstrated procurvatum proximally, and recurvatum distally in the sagittal plane, but showed no difference in the frontal plane. FDD radii possessed excessive recurvatum proximally, and procurvatum distally in the sagittal plane, and varus proximally and valgus distally in the frontal plane. Whereas no torsion was discernible in the humeri, all radii had external torsion. In the frontal plane, FDD femurs exhibited varus both proximally and distally whereas the tibia possessed proximal valgus and distal varus. No torsion in the pelvic limbs was observed. No spinal pathology was detected in the FDD cats included in the original study.

Conclusion—Feline disproportionate dwarfism results in significant appendicular deformity in all limbs. The incidence of intervertebral disc degeneration in FDD cats is inconclusive.

Address for correspondence Derek B. Fox, DVM, PhD, DACVS, Veterinary Medical Health Center, University of Missouri, 900 East Campus Drive, Columbia, MO 65211, United States (FoxDB@missouri.edu).

Authors' Contributions

L.M.A., D.B.F., and J.R.C. contributed to conception of study, study design, acquisition of data, data analysis and interpretation and manuscript preparation. K.L.C. contributed to conception of study and acquisition of data. B.T.T. contributed to statistical analysis and manuscript preparation. L.A.L. contributed to concept of study, study design, acquisition of data and manuscript preparation. All authors drafted, revised, and approved the submitted manuscript.

Conflict of Interest

L.M.A. reports grants from Gilbreath-McLorn Endowment, during the conduct of the study. The other authors report no conflict of interest.

Keywords

chondrodysplasia; Munchkin cat; disproportionate dwarfism; joint orientation angles; angular limb deformities

Introduction

The term *chondrodystrophy* was introduced by Hansen to describe dogs with both shortening of the limbs and premature degeneration of the intervertebral discs.[1,2] Chondrodystrophy is now frequently used interchangeably with the descriptor *disproportionate dwarfism* to describe dogs possessing a skeletal dysplasia in which the limbs are shortened despite having a proportionately sized cranium and axial skeleton. Although disproportionate dwarfism is considered pathologic in humans, similar chondrodysplasias are selected for in several domesticated breeds of animals. Canine chondrodysplasia, the short-legged phenotype identified in at least 19 dog breeds, is a result of an autosomal recessive retrogene, encoding *fibroblast growth factor 4* (*FGF4*), which is inserted on either chromosome 12 or 18.[3-5] Musculoskeletal ramifications of the mutation can include intervertebral disc disease and characteristic limb shortening and malalignment.[3-6] Additionally, mutations in other genes, including cartilage specific integrin α 10, have been identified in some forms of canine disproportionate dwarfism.[7]

Feline disproportionate dwarfism (FDD) is now under positive selection in breeds of cats alternatively referenced as *Munchkin, Minuet* and *Napoleon.* This phenotype was recognized and approved by The International Cat Association in 1995. Genetic studies suggest a form of FDD is caused by a novel autosomal dominant dwarfism gene, *UDP-glucose 6-dehydrogenase* (*UGDH*).[8-10] However, FDD cats appear to be similar in phenotype to dogs affected by disproportionate dwarfism with respect to a grossly shortened stature (Fig. 1). Because of the different genetic etiopathogenesis, FDD cats may demonstrate different skeletal manifestations compared with chondrodystrophic dogs.

Limb alignment is successfully evaluated using the center of rotation of angulation (CORA) methodology of radiograph interpretation, first adapted from human medicine and applied to dogs in 2006.[11] Since that time, the CORA methodology has been used to determine a reference library of radiographic normal axes, joint orientation lines (JOL) and joint orientation angles (JOA) for the humerus, radius and ulna, femur and tibia in dogs,[11-17] and the femur and tibia in cats.[18] This methodology has also been used to characterize and classify deformities in both thoracic and pelvic limbs in dogs.[19-27] Magnetic resonance imaging (MRI) is considered the diagnostic modality of choice for the examination of the spinal cord and for early detection of intervertebral disc degeneration, common in chondrodysplastic dogs.[6,28] Magnetic resonance imaging findings consistent with disc degeneration, bulging discs, disc protrusions and extrusions have been well described.[29]

No descriptions of the specific axial and appendicular skeletal manifestations affecting FDD cats are published. The first objective was to characterize the radiographic alignment of FDD thoracic and pelvic limbs compared with normal cats using the CORA methodology. The second objective was to evaluate for the presence or absence of intervertebral disc

disease in FDD cats using MRI. There were two hypotheses. First, FDD cats would demonstrate characteristic constellations of appendicular skeletal malalignment compared with unaffected cats discernible by significant differences in measured JOA. Second, FDD cats would not be predisposed to early intervertebral disc degeneration as evidenced by signal hyperintensity on T2-weighted images.

Materials and Methods

Sample Population

All procedures were performed with an approved University of Missouri Institutional Animal Care and Use Committee protocol (ACUC protocol # 9642) following institutional guidelines. Skeletally mature domestic short hair cats (n = 12) from a University of Missouri research colony served as a normal population of thoracic limbs. The cats had mixed breed origins, including contributions from Persian, Bengal, Burmese, American curl, Toyger and Japanese bobtail. Exclusion criteria included cats that were skeletally immature, had a history of lameness or trauma or demonstrated evidence of orthopaedic or neurologic disease. Six privately owned FDD cats confirmed to have the UGDH structural variant via genetic analysis represented the affected group whose owners provided informed consent for the completion of examinations, radiography and/or MRI (Table 1).

Normal Thoracic Limb Assessment

Cats were sedated with dexmedetomidine (Dexdomitor, Zoetis, Parsippany, New Jersey, United States) at 5 μg/kg intravenous (IV) once. Frontal plane (craniocaudal) and sagittal plane (mediolateral) digital radiographs were obtained for each forelimb extending from the distal scapula through the phalanges. Limb position was standardized by prioritizing a straight view of the elbow in both frontal and sagittal planes. Elbow position was standardized in the frontal plane by assessing the elbow rotational position.[12] In the sagittal plane, radiographic positioning was standardized by drawing best fit circles over medial and lateral parts of the humeral condyle and aligning the humerus so that the circles were concentric and not intersecting.[13] Limb alignment was assessed using commercially available software (eFilm Workstation, IBM Watson Health, Armonk, New York, United States).

The mechanical axis was used in conjunction with the JOL for both shoulder and elbow to assess the humerus in the frontal and sagittal planes.[13] Briefly, for the frontal plane, the center of a best-fit oval over the humeral head and mid-point of the articular surface of the humeral condyle along the elbow JOL served as proximal and distal landmarks. In the sagittal plane, the center of the best-fit oval over the humeral head and best-fit circle drawn over the lateral humeral condyle served as landmarks (Fig. 2).

Anatomic axes and JOL for both elbow and carpus were used to assess alignment of the radius in the frontal and sagittal planes.[30] In the frontal plane, a best fit line bisecting the radius at the proximal and distal metaphysis represented the anatomic axis. In the sagittal plane, two anatomic axes exist due to the natural procurvatum and were represented by two best fit lines bisecting the proximal and distal radius (Fig. 3).[30]

The intersecting angles between respective anatomic (radius) or mechanical (humerus) axes and JOL were measured and recorded as a set of JOA (Table 2), including the mean, standard deviation and 95% confidence interval. All measurements were performed in triplicate by a single investigator (KLC).

Normal Pelvic Limb Assessment

Swanson and colleagues[18] previously applied the CORA methodology to assess and determine the normal pelvic limb JOA in the frontal plane of skeletally mature mixed breed cats.[14,15] Briefly, a line from the center of the femoral head bisecting the proximal aspect of the intercondylar fossa served as the mechanical axis of the femur. The mechanical axis of the tibia was defined by a line from the proximal aspect of the femoral intercondylar fossa through the distal point of the intermediate tibial ridge. Intersecting angles between respective axes and JOL were used to establish mean JOA values (Table 3; Fig. 4). The dataset from the Swanson and colleagues[18] study (n = 100 limbs) was retrieved and used as reference standards for statistical comparison with our FDD dataset. The study included 50 skeletally mature domestic short hair cats (26 male, 24 female).

Appendicular Skeletal Deformity Classification in Feline Disproportionate Dwarfism Cats

Privately owned cats identified by a breeder as demonstrating FDD (n = 5) were radiographically evaluated. Full limb radiographs were taken for each FDD cat. Upon physical examination, a torsional deformity of the antebrachium was present in all cats. Thus, positioning was standardized in the thoracic limb by achieving both an elbow straight view and a carpal straight view in the frontal and sagittal planes to mitigate the radiographic artifacts associated with torsional deformities.[30,31] Pelvic limb positioning was standardized by achieving a stifle-straight view in the frontal plane.[18]

The JOA for the humerus and radius in both the frontal and sagittal planes were measured using the CORA methodology described above. For the radius, an elbow-straight view was used for the determination of the proximal JOA, and a carpal straight view was used to define the distal JOA. Similarly, the JOA were determined for the femur and tibia in the frontal plane using the method described by Swanson and colleagues[18] All measurements were performed in triplicate by a single investigator (LMA). The dataset for each JOA was used to calculate the mean, standard deviation and 95% confidence interval, then compared with respective normal JOA. Differences were characterized descriptively as either varus or valgus deformities in the frontal plane, and procurvatum or recurvatum deformities in the sagittal plane. Torsional deformities were labelled as being absent or having external or internal torsion based on physical examination.

Intervertebral Disc Assessment

Two skeletally mature FDD cats were sedated with dexmedetomidine (Dexdomitor, Zoetis, Parsippany, New Jersey, United States) at 5 μg/kg IV and anesthetized by propofol (Propofol, Pfizer, New York, New York, United States) at 4 mg/kg IV; anaesthesia was maintained with isoflurane (Isoflurane USP, Piramal Healthcare, Bethlehem, Pennsylvania, United States) at 2%. The cats were positioned in sternal recumbency. Magnetic resonance imaging of the cervical, thoracic, lumbar and sacral spinal regions (T3 through sacrum)

was performed with a 3-Tesla unit (Toshiba/Canon 3T MR scanner). Pulse sequences were selected to obtain T2-weighted sequences in three planes. The images were evaluated by a board-certified veterinary neurologist (JRC). Cats were classified as having disc degeneration if structurally inhomogeneous nucleus pulposus, inhomogeneous, grey or black intervertebral disc space, loss of distinction between the annulus fibrosis and nucleus pulposus and/or decreased width of the disc space were noted.[29]

Statistical Analysis

Analyses were performed using statistical software (GraphPad Prism version 8.3.1 for MacOS, GraphPad Software, San Diego, California, United States, www.graphpad.com). Descriptive statistics were compiled for each variable and means ± standard deviation and 95% confidence intervals were determined. Normality was determined with the D'Agostino and Pearson test. A paired-t test was used to determine differences in the individual normal cat outcome variables between right and left limbs. If no significant differences were found, the data from the right and left limbs were combined for statistical comparison. This was repeated for the FDD dataset. Comparisons between normal and FDD variables was performed with an unpaired-t test with Welch's correction. Significance for all comparisons was set at $p \leq 0.05$.

Results

Normal Thoracic Limb Assessment

Twenty-four thoracic limbs from 12 skeletally mature domestic short hair cats were analysed. The mixed breed cats were considered moderate for body and limb type. No difference was found between the triplicate measurements ($p = 0.90$) or between the left and right limb measurements ($p = 0.07$). The 24 measurements were pooled and the mechanical JOA for the humerus and anatomic JOA for the radius (Table 4) are summarized.

Feline Disproportionate Dwarfism Cats

Six FDD cats were included in the study, including four males and two females. Genetic analysis confirmed that all cats possessed the UGDH variant. The signalment of the FDD cats is summarized in Table 1.

Feline Disproportionate Dwarfism Thoracic Limb Assessment

Ten thoracic limbs from five skeletally mature FDD cats were analysed both grossly and radiographically. No significant differences were found between the right and left limb measurement. The JOA for the humerus and radius and the statistical comparison to normal JOA angles are summarized in Table 4. In the sagittal plane, the humerus exhibited proximal procurvatum (mCdPHA = 46 degrees [$p < 0.001$]) and distal recurvatum (mCrDHA = 83 degrees [$p = 0.041$]) resulting in an exaggerated sigmoidal shape in the sagittal plane compared with normal cats (Fig. 5). No differences were found in the frontal plane alignment of the humerus between normal and FDD cats (mLDHA = 84 degrees [$p = 0.08$]). Based on visual examination of the cats and radiographic evaluation of the elbow and shoulder joint, no torsional deformities were present in the FDD humeri.

Data from two frontal plane antebrachia could not be collected due to excessive antebrachial torsion and an inability to capture straight-elbow positioned radiographs according to the predetermined elbow rotational position standardization.[12] In the frontal plane, the FDD radius possessed partially compensatory changes characterized by proximal radial varus (aMPRA = 75 degrees [$p = 0.009$]) and distal radial valgus (aLDRA = 82 degrees [$p < 0.001$]) (Fig. 6). In the sagittal plane, excessive recurvatum proximally (aCrPRA = 63 degrees [$p < 0.001$]) and procurvatum distally (aCdDRA = 87 degrees [$p < 0.001$]) was detected (Fig. 6). Further, external torsion of the antebrachium was present in all limbs evaluated.

Feline Disproportionate Dwarfism Pelvic Limb Assessment

Ten pelvic limbs from five skeletally mature FDD cats were analysed. No significant differences were found between the right and left limb measurements. The mechanical JOA for the femur and tibia and the comparison to normal JOA are summarized in Table 5. Significantly different proximal ($p < 0.001$) and distal ($p = 0.009$) JOA revealed a reduction in the femoral inclination angle, or coxa vara, proximally (mLPFA = 106 degrees) and femoral varus distally (mLDFA = 103.5 degrees) (Fig. 7). Further, significant differences in both proximal ($p < 0.001$) and distal ($p < 0.001$) JOA of the FDD tibia resulting in proximal tibial valgus (mMPTA = 97 degrees) and distal tibial varus (mMDTA = 96 degrees) were observed. No torsional deformities were present in either the femur or tibia.

Evaluation of the Intervertebral Discs

One female spayed 4-year-old FDD cat and 1 male castrated 9-year-old FDD cat underwent spinal MRI. All intervertebral discs were T2-weighted hyperintense and in normal anatomic position (Fig. 8A).

Discussion

This study reported the morphologic changes in the axial and appendicular skeletons of cats associated with disproportionate dwarfism attributable to the structural UGDH variant. Further, reference values for JOA in normal feline thoracic limb using standardized methods are presented. The alterations in limb alignment associated with FDD cats compared with normal populations were characterized using the CORA methodology. The FDD cats had complex antebrachial malalignment consisting of proximal radial varus, distal radial valgus and external torsion similar to chondrodystrophic dogs.[19] Additional deformities in the sagittal plane of the thoracic limb were evidenced by the presence of exaggerated sigmoidal shapes of both the humerus and radius. The pelvic limbs also demonstrated significant differences from previously established normal parameters, including femoral coxa vara, distal femoral varus, proximal tibial valgus and distal tibial varus.

Humeral malalignment of FDD cats was limited to the sagittal plane. Smith and colleagues[32] previously compared the sagittal alignment of the humerus in non-chondrodystrophic dogs to chondrodystrophic dogs and found no significant differences, highlighting a difference between chondrodystrophic dogs and FDD cats. The clinical relevance of subtle angular changes in the sagittal plane of the humerus is not known but is suspected to be minimal as

quadrupeds are able to compensate for such malalignment through alteration of the standing angle of both the shoulder and elbow.

The antebrachia of FDD cats demonstrated characteristic malalignment similar to chondrodystrophic dogs—biapical partially compensated deformities.[19] These deformities have been associated with gait abnormalities and concurrent joint disease of the elbow and carpus in dogs.[30] Chondrody-strophic dogs are 3.5 times more likely to have elbow disease than non-chondrodystrophic breeds including elbow osteoarthritis and lateral radial head subluxation.[19,21,30] Due to the prevalence of joint disease in dogs with malalignment, the malalignment in the frontal plane of FDD cats may increase the likelihood for the development of secondary osteoarthritis. While no gross radiographic evidence of osteoarthritis existed in this population of FDD cats, it would be presumptuous to conclude what effects FDD-related malalignment might have on joint health over the life of an affected cat based on radiography alone in such a small population of relatively young animals.

The pelvic limbs of FDD cats possess a constellation of specific malalignment changes, that when present in dogs, can be associated with medial patellar luxation.[33] Specifically, dogs with high grade patellar luxation are increasingly identified as possessing femorotibial malalignment. Pelvic limb alignment has not been evaluated in cases of feline congenital patellar luxation. However, the clinical ramifications of the identified differences in alignment are unknown in the FDD cat.

All cats in the FDD cohort were determined to possess the UGDH genetic variant. The UGDH gene encodes an oxidoreductase enzyme that converts UDP-glucose to UDP-glucuronic acid.[34] UDP-glucuronic acid is an essential sugar nucleotide which serves as a precursor and regulator of several sulphated glycosaminoglycans.[35] Proteoglycans comprised of such glycosaminoglycans are critical to the regulation of many types of growth factors including those in the FGF family.[36] As such, mutation of the UGDH gene in embryonic mice has been shown to block normal FGF signaling.[36] FGF is involved in embryonal development and is critical for normal limb formation across species.[37] Related, canine chondrodystrophy results from aberrant FGF production, although the source of excess production is via FGF retrogene insertions.[6] While it remains unknown if FDD cats demonstrate abnormal limb development secondary to UGDH-based dysregulation of proteoglycan-FGF signaling,[10] the potential connection between UGDH variants and FGF deserves further examination. Musculoskeletal sequela of loss-of-function UGDH in humans does not appear to result in similar limb dysgenesis, but can result in mild facial dysmorphism, axial hypotonia and neurologic signs attributable to encephalopathy.[38]

In general, the incidence of feline thoracolumbar intervertebral disc disease is rare compared with dogs with an incidence of 0.24% in a report evaluating 12,900 cats.[39] Chondrodystrophic dogs are at a particularly high risk for intervertebral disc degeneration due to chondroid metaplasia leading to mineralization and premature degeneration.[6] Chondroid metaplasia is strongly associated with the *FGF4* retrogene insertion in chondrodystrophic dogs.[6] It is unknown what effect the UDGH variant has on the health of intervertebral discs in affected cats. Based on the results of MRI analysis of two FDD

cats, the initial supposition of this study was that this particular UDGH variant did not result in premature intervertebral disc degeneration. However, in the time since completion of the study, a clinical case of a 6-year-old female spayed FDD cat presented to our hospital with an acute history of paraparesis. The cat was subsequently diagnosed with multifocal intervertebral disc degeneration and a single site of disc herniation between the 4th and 5th lumbar vertebral bodies identified on MRI (Fig. 8B). Based on this occurrence, it cannot be ruled out that the UDGH variant responsible for the described skeletal dysplasia might also affect the health of intervertebral discs. This further emphasizes the need for comprehensive longitudinal studies to be performed documenting the progression of both joint and intervertebral disc health over the life of FDD cats.

The current study possessed several limitations. Most importantly, only six FDD cats were evaluated. This small population size may explain the relatively large confidence interval for FDD JOA. However, the breeder was asked to present the shortest and longest legged cats from her cattery. The wide range may also be secondary to phenotypic variation of the *UGDH* variant responsible for this type of feline dwarfism. Cats with the same DNA variant can have highly variable presentation; thus, genetic and environmental modifiers are suspected to affect the degree of deformities. With the small population evaluated, it was not possible to draw correlations between the degrees of limb shortening to the severity of malalignment.

A segmental orthogonal radiographic technique was employed to mitigate radiographic artifact that has been associated with torsion–angulation deformities for the FDD antebrachia. While this method has been validated, miscalculations of the alignment when torsional angulation exceeds 15 degrees have been shown.[30] Related, there was difficulty obtaining elbow-straight views of two FDD antebrachia due to severe external torsion and the small size of the animals. These two elbows were not considered straight in the frontal plane when radiographs were critiqued using the elbow rotational position methodology[12] and were necessarily excluded from the analysis. To more accurately assess deformities in the transverse plane and minimize miscalculations in frontal and sagittal plane radiographs associated with torsion–angulation deformities, future studies may benefit from computed tomographic evaluations.[12]

Despite these limitations, this work serves as the first to define the skeletal manifestations of FDD cats and distinguish them from canine chondrodystrophy. Significant appendicular skeletal alignment differences exist compared with normal cats. Although not evaluated here, such malalignment likely alters biomechanical loading across the respective joints which may affect joint health over the lifetime of affected cats. Importantly, there is some evidence suggesting FDD may affect the axial skeleton. Future studies should evaluate larger numbers of affected cats of varying age ranges and phenotypic expression to further define potential FDD related skeletal changes.

Funding

This research was funded in full by Gilbreath-McLorn Endowment. The research funder was not involved in any other aspect of the study.

References

1. Hansen HJ. A pathologic-anatomical study on disc degeneration in dog, with special reference to the so-called enchondrosis intervertebralis. Acta Orthop Scand Suppl 1952;11:1–117 [PubMed: 14923291]
2. Hansen HJ. A pathologic-anatomical interpretation of disc degeneration in dogs. Acta Orthop Scand 1951;20(04):280–293 [PubMed: 14894198]
3. Parker HG, VonHoldt BM, Quignon P, et al. An expressed fgf4 retrogene is associated with breed-defining chondrodysplasia in domestic dogs. Science 2009;325(5943):995–998 [PubMed: 19608863]
4. Brown EA, Dickinson PJ, Mansour T, et al. *FGF4* retrogene on CFA12 is responsible for chondrodystrophy and intervertebral disc disease in dogs. Proc Natl Acad Sci U S A 2017;114(43):11476–11481 [PubMed: 29073074]
5. Murphy BG, Dickinson P, Marcellin-Little DJ, Batcher K, Raverty S, Bannasch D. Pathologic features of the intervertebral disc in young Nova Scotia Duck Tolling Retrievers confirms chondrodystrophy degenerative phenotype associated with genotype. Vet Pathol 2019;56(06):895–902 [PubMed: 31526126]
6. Batcher K, Dickinson P, Giuffrida M, et al. Phenotypic effects of FGF4 retrogenes on intervertebral disc disease in dogs. Genes (Basel) 2019;10(06):435 [PubMed: 31181696]
7. Kyöstilä K, Lappalainen AK, Lohi H. Canine chondrodysplasia caused by a truncating mutation in collagen-binding integrin alpha subunit 10. PLoS One 2013;8(09):e75621 [PubMed: 24086591]
8. Lyons LA, Fox DB, Chesney KL, et al. Localization of a feline autosomal dominant dwarfism locus: a novel model of chondrodysplasia. BioRxiv 2019. Doi: 10.1101/687210
9. Buckley RM, Davis BW, Brashear WA, et al. A new domestic cat genome assembly based on long sequence reads empowers feline genomic medicine and identifies a novel gene for dwarfism. BioRxiv 2020. Doi: 10.1101/2020.01.06.896258
10. Struck AK, Braun M, Detering KA, et al. A structural UGDH variant associated with standard Munchkin cats. BMC Genet 2020;21(01):67 [PubMed: 32605545]
11. Fox DB, Tomlinson JL, Cook JL, Breshears LM. Principles of uniapical and biapical radial deformity correction using dome osteotomies and the center of rotation of angulation methodology in dogs. Vet Surg 2006;35(01):67–77 [PubMed: 16409412]
12. Fasanella FJ, Tomlinson JL, Welihozkiy A, et al. Radiographic measurements of the axes and joint angles of the canine radius and ulna. Vet Comp Orthop Traumatol 2010;23:A11
13. Wood MC, Fox DB, Tomlinson JL. Determination of the mechanical axis and joint orientation lines in the canine humerus: a radiographic cadaveric study. Vet Surg 2014;43(04):414–417 [PubMed: 24617644]
14. Tomlinson J, Fox D, Cook JL, Keller GG. Measurement of femoral angles in four dog breeds. Vet Surg 2007;36(06):593–598 [PubMed: 17686134]
15. Dismukes DI, Tomlinson JL, Fox DB, Cook JL, Song KJE. Radiographic measurement of the proximal and distal mechanical joint angles in the canine tibia. Vet Surg 2007;36(07):699–704 [PubMed: 17894597]
16. Dismukes DI, Tomlinson JL, Fox DB, Cook JL, Witsberger TH. Radiographic measurement of canine tibial angles in the sagittal plane. Vet Surg 2008;37(03):300–305 [PubMed: 18394079]
17. Dismukes DI, Fox DB, Tomlinson JL, Cook JL, Essman SC. Determination of pelvic limb alignment in the large-breed dog: a cadaveric radiographic study in the frontal plane. Vet Surg 2008;37(07):674–682 [PubMed: 19134090]
18. Swanson EA, Tomlinson JL, Dismukes DI, Fox DB. Measurement of femoral and tibial joint reference angles and pelvic limb alignment in cats. Vet Surg 2012;41(06):696–704 [PubMed: 22823144]
19. Knapp JL, Tomlinson JL, Fox DB. Classification of angular limb deformities affecting the canine radius and ulna using the center of rotation of angulation method. Vet Surg 2016;45(03):295–302 [PubMed: 27011252]

20. Dismukes DI, Fox DB, Tomlinson JL, Essman SC. Use of radiographic measures and three-dimensional computed tomographic imaging in surgical correction of an antebrachial deformity in a dog. J Am Vet Med Assoc 2008;232(01):68–73 [PubMed: 18167111]
21. Kwan TW, Marcellin-Little DJ, Harrysson OL. Correction of biapical radial deformities by use of bi-level hinged circular external fixation and distraction osteogenesis in 13 dogs. Vet Surg 2014;43(03):316–329 [PubMed: 24410998]
22. Fitzpatrick N, Nikolaou C, Farrell M, et al. The double-arch modified type-1b external skeletal fixator. Technique description and functional outcome for surgical management of canine antebrachial limb deformities. Vet Comp Orthop Traumatol 2011;24(05):374–382 [PubMed: 21822528]
23. Lesser AS, Maguire PJ. Clinical implementation of a novel osteotomy of the radius to correct biapical canine angular limb deformities. Vet Surg 2014;43:177–178
24. Yasukawa S, Edamura K, Tanegashima K, et al. Evaluation of bone deformities of the femur, tibia, and patella in Toy Poodles with medial patellar luxation using computed tomography. Vet Comp Orthop Traumatol 2016;29(01):29–38 [PubMed: 26638694]
25. Dudley RM, Kowaleski MP, Drost WT, Dyce J. Radiographic and computed tomographic determination of femoral varus and torsion in the dog. Vet Radiol Ultrasound 2006;47(06):546–552 [PubMed: 17153063]
26. DeTora MD, Boudrieau RJ. Complex angular and torsional deformities (distal femoral malunions). Preoperative planning using stereolithography and surgical correction with locking plate fixation in four dogs. Vet Comp Orthop Traumatol 2016;29(05):416–425 [PubMed: 27439728]
27. Apelt D, Kowaleski MP, Dyce J. Comparison of computed tomographic and standard radiographic determination of tibial torsion in the dog. Vet Surg 2005;34(05):457–462 [PubMed: 16266337]
28. Brisson BA. Intervertebral disc disease in dogs. Vet Clin North Am Small Anim Pract 2010;40(05):829–858 [PubMed: 20732594]
29. Besalti O, Pekcan Z, Sirin YS, Erbas G. Magnetic resonance imaging findings in dogs with thoracolumbar intervertebral disk disease: 69 cases (1997-2005). J Am Vet Med Assoc 2006;228(06):902–908 [PubMed: 16536704]
30. Fox DB, Tomlinson JL. Principles of angular limb deformity correction. In: Tobias KM, Johnston SA, eds. Veterinary Surgery: Small Animal. 2nd edition St. Louis: Elsevier; 2018: 762–774
31. Piras LA, Peirone B, Fox D. Effects of antebrachial torsion on the measurement of angulation in the frontal plane: a cadaveric radiographic analysis. Vet Comp Orthop Traumatol 2012;25(02):89–94 [PubMed: 22286804]
32. Smith EJ, Marcellin-Little DJ, Harrysson OLA, Griffith EH. Influence of chondrodystrophy and brachycephaly on geometry of the humerus in dogs. Vet Comp Orthop Traumatol 2016;29(03):220–226 [PubMed: 27070343]
33. Di Dona F, Della Valle G, Fatone G. Patellar luxation in dogs. Vet Med (Auckl) 2018;9:23–32 [PubMed: 30050864]
34. Alhamoudi KM, Bhat J, Nashabat M, et al. A missense mutation in the UGDH gene is associated with developmental delay and axial hypotonia. Front Pediatr 2020;8:71 [PubMed: 32175296]
35. Zhang L Glycosaminoglycan (GAG) biosynthesis and GAG-binding proteins. Prog Mol Biol Transl Sci 2010;93:1–17 [PubMed: 20807638]
36. García-García MJ, Anderson KV. Essential role of glycosaminoglycans in Fgf signaling during mouse gastrulation. Cell 2003;114(06):727–737 [PubMed: 14505572]
37. Lu P, Minowada G, Martin GR. Increasing Fgf4 expression in the mouse limb bud causes polysyndactyly and rescues the skeletal defects that result from loss of Fgf8 function. Development 2006;133(01):33–42 [PubMed: 16308330]
38. Hengel H, Bosso-Lefèvre C, Grady G, et al. Loss-of-function mutations in UDP-Glucose 6-Dehydrogenase cause recessive developmental epileptic encephalopathy. Nat Commun 2020;11(01):595. Doi: 10.1038/s41467-020-14360-7 [PubMed: 32001716]
39. De Decker S, Warner AS, Volk HA. Prevalence and breed predisposition for thoracolumbar intervertebral disc disease in cats. J Feline Med Surg 2017;19(04):419–423 [PubMed: 26868632]

Fig. 1.
Feline disproportionate dwarfism (FDD). FDD cat demonstrating a disproportionally short stature associated with the phenotype of the feline dwarf breed.

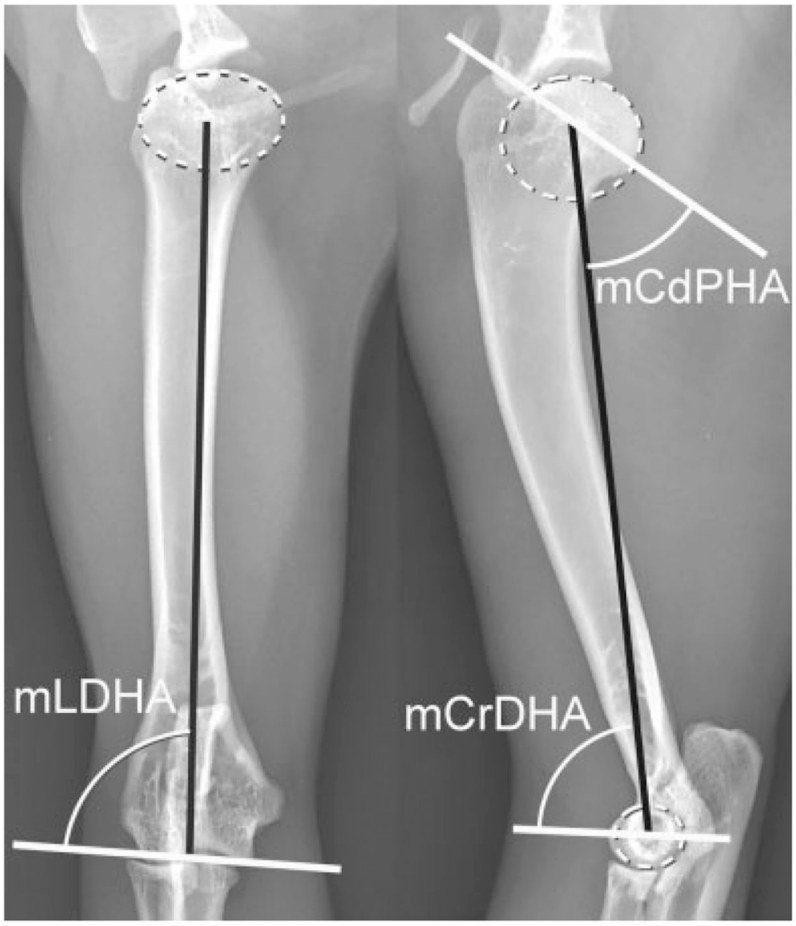

Fig. 2.

Normal cat humerus. Best fit ovals and circles (dotted white oval and circle) placed over the humeral head and the lateral humeral condyle respectively to determine the center of the humeral head and lateral condyle respectively. Joint orientation lines (solid white lines) and the mechanical axis (solid black lines) with associated joint orientation angles used to evaluate the humerus in the frontal and sagittal planes. mCdPHA, mechanical caudal proximal humeral angle; mCrDHA, mechanical cranial distal humeral angle; mLDHA, mechanical lateral distal humeral angle.

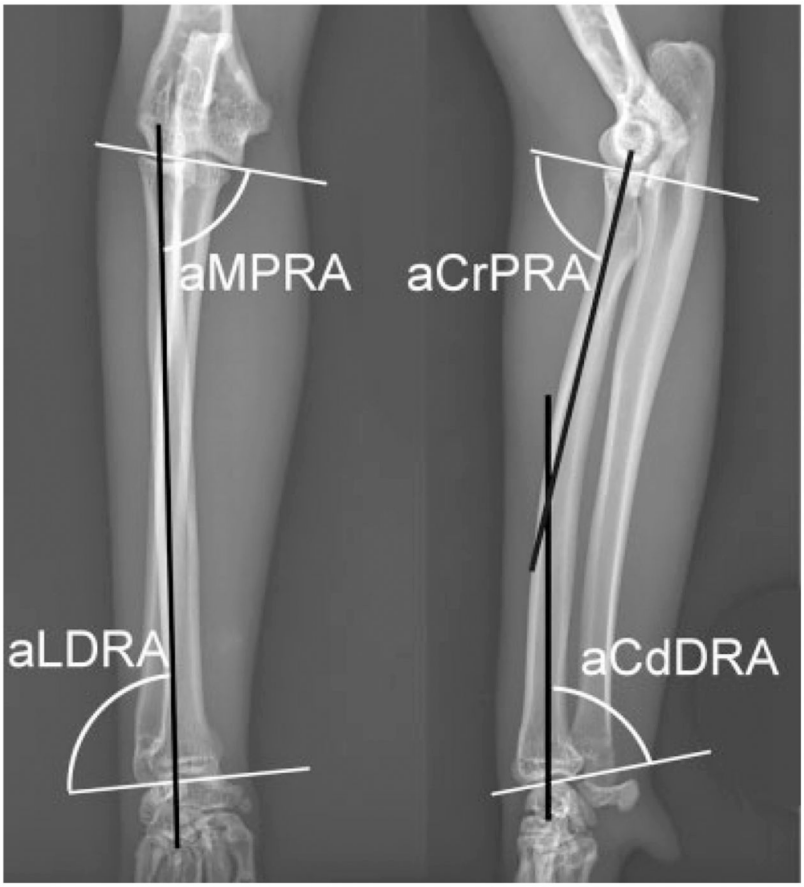

Fig. 3.

Normal cat radius. Joint orientation lines (solid white lines) and the anatomic axes (solid black lines) with associated joint orientation angles used to evaluate the radius in the frontal and sagittal planes. aCdDRA, anatomic caudal distal radial angle; aCrPRA, anatomic cranial proximal radial angle; aLDRA, anatomic lateral distal radial angle; aMPRA, anatomic medial proximal radial angle.

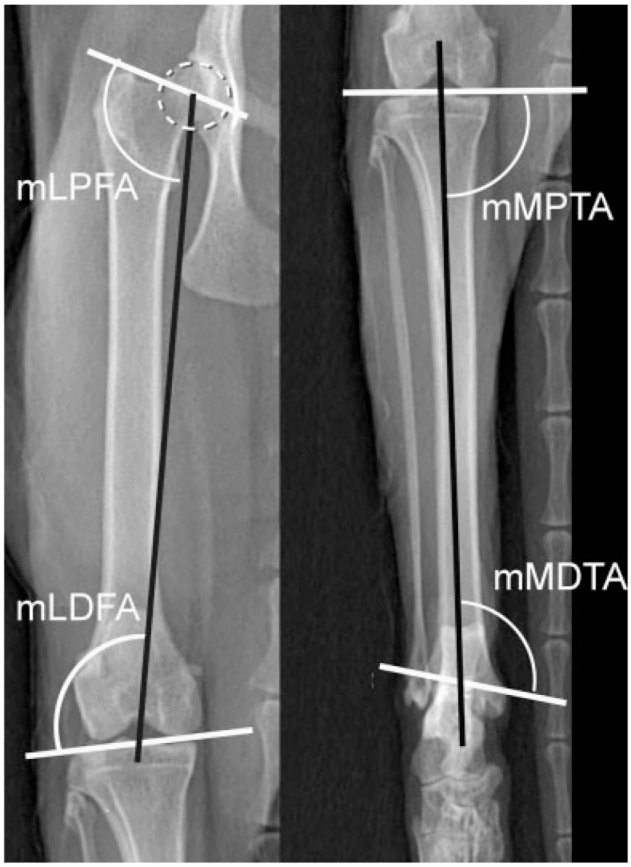

Fig. 4.

Normal cat femur and tibia. The best fit circle over the femoral head (dotted white circle) is used to determine the center of the femoral head. Joint orientation lines (solid white lines) and the mechanical axis (solid black lines) with associated joint orientation angles used to evaluate the femur and tibia in the frontal plane. mLDFA, mechanical lateral distal femoral angle; mLPFA, mechanical lateral proximal femoral angle; mMDTA, mechanical medial distal tibial angle; mMPTA, mechanical medial proximal tibial angle.

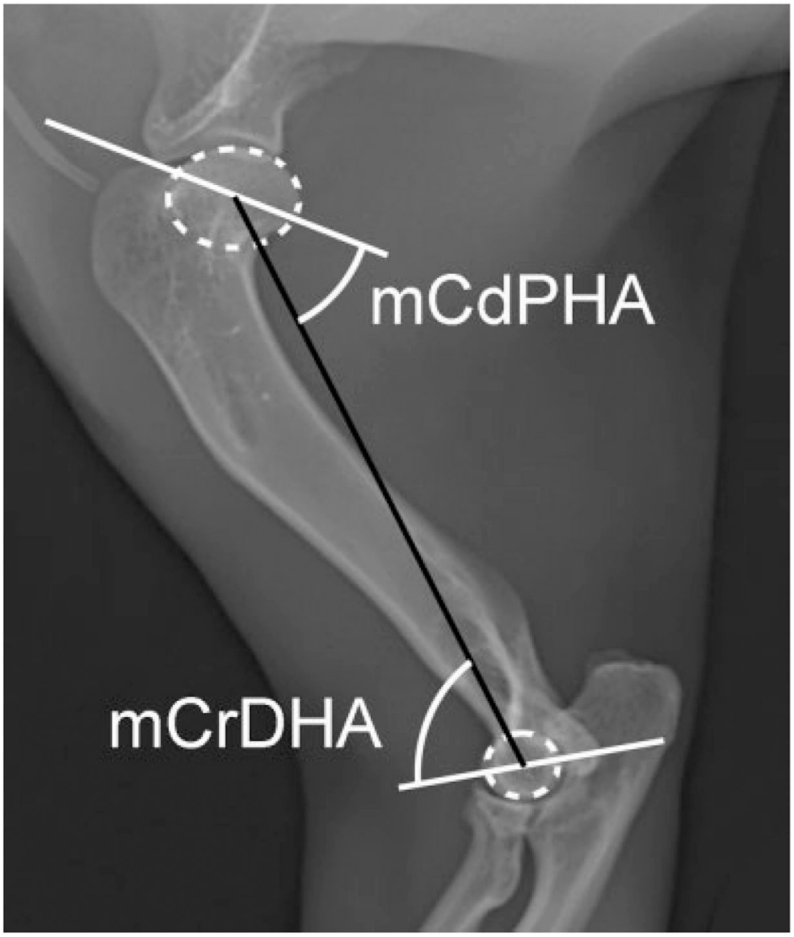

Fig. 5.

Feline disproportionate dwarfism cat humerus. Best fit ovals (dotted white oval) placed over the humeral head and the lateral humeral condyle to determine the center of the head and lateral condyle. Joint orientation lines (solid white lines) and the mechanical axis (solid black line) with associated joint orientation angles used to evaluate the humerus in the sagittal plane. The humerus has a significantly smaller mCdPHA and larger mCrDHA compared with normal cats resulting in an exaggerated sigmoid shape in the sagittal plane characterized by proximal procurvatum and distal recurvatum. mCdPHA, mechanical caudal proximal humeral angle; mCrDHA, mechanical cranial distal humeral angle.

Fig. 6.

Feline disproportionate dwarfism cat radius. Joint orientation lines (solid white lines) and the anatomic axes (solid black lines) with associated joint orientation angles used to evaluate the radius in the frontal and sagittal planes. The radius is characterized by a smaller aMPRA described as proximal radial varus (**A**), a smaller aLDRA described as distal radial valgus (**B**), smaller aCrPRA described as excessive proximal recurvatum (**C**) and larger aCdDRA described as distal excessive distal procurvatum (**D**) compared with normal cats. aCdDRA, anatomic caudal distal radial angle; aCrPRA, anatomic cranial proximal radial angle; aLDRA, anatomic lateral distal radial angle; aMPRA, anatomic medial proximal radial angle.

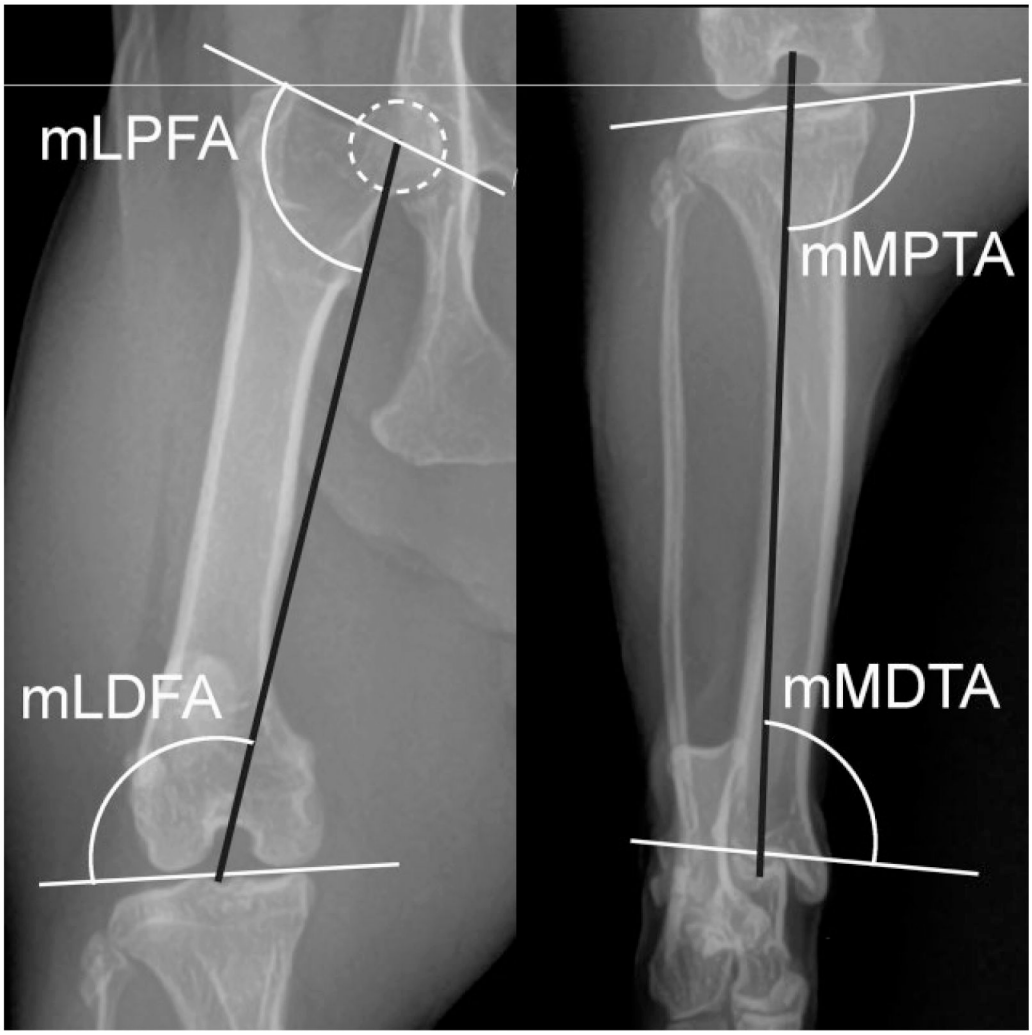

Fig. 7.

Feline disproportionate dwarfism (FDD) cat femur and tibia. The best fit circle over the femoral head (dotted white circle) is used to determine the center of the femoral head. Joint orientation lines (solid white lines) and the mechanical axis (solid black lines) with associated joint orientation angles used to evaluate the femur and tibia in the frontal plane. The femur is characterized by a larger mLPFA resulting in coxo vara, and distal femoral varus as a result of a larger mLDFA compared with normal cats. The FDD tibia is characterized by proximal tibial valgus as seen by a larger mMPTA and distal tibial varus as seen by a smaller mMDTA compared with normal cats. mLDFA, mechanical lateral distal femoral angle; mLPFA, mechanical lateral proximal femoral angle; mMDTA, mechanical medial distal tibial angle; mMPTA, mechanical medial proximal tibial angle.

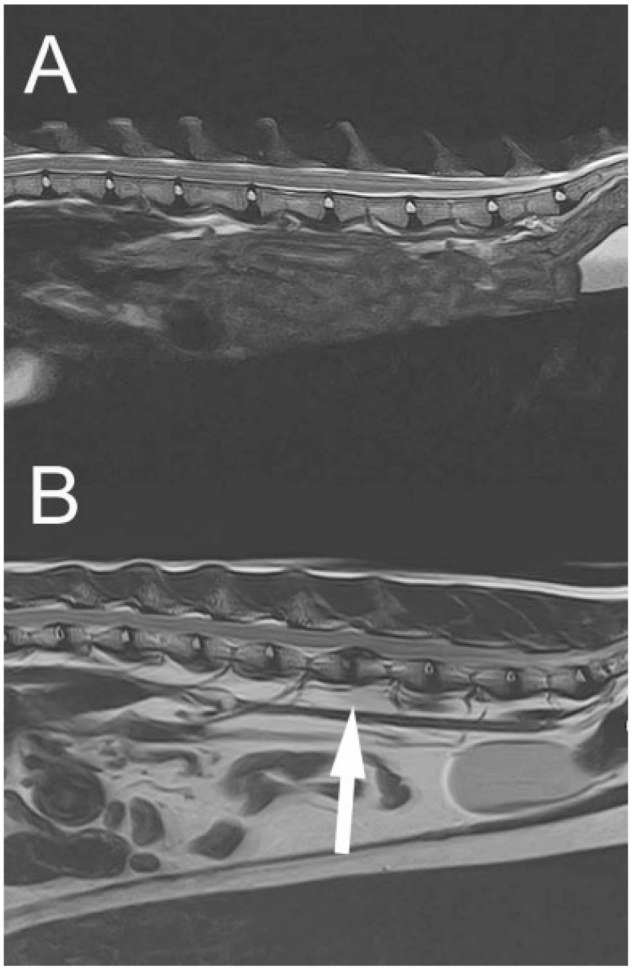

Fig. 8.

(**A**) A 9-year-old female, feline disproportionate dwarfism cat thoracolumbar magnetic resonance imaging (MRI). Representative T2-weighted spinal MRI extending from T13 through the sacrum; note the T2 hyperintensity of the nucleus pulposus in normal anatomical positions. (**B**) A 6-year-old female spayed, feline disproportionate dwarfism cat thoracolumbar MRI. Representative T2-weighted spinal MRI. Note the variable T2 hypointensity of the nuclei pulposi and the dorsally herniated nucleus pulposus between the 4th and 5th lumbar vertebral bodies (white arrow) causing spinal cord compression.

Table 1

Description of the feline disproportionate dwarfism (FDD) cats included for radiographic and magnetic resonance imaging (MRI) analysis

FDD cat	Age (y)	Sex	Weight (kg)	Diagnostic evaluation
1	9	Female	2.4	Radiographs, MRI
2	2	Male	3.8	Radiographs
3	1	Male	2.8	Radiographs
4	1.5	Female	1.8	Radiographs
5	1	Male	2.5	Radiographs
6	5	Male	2.9	MRI

Table 2

Nomenclature of joint orientation angles measured in the frontal and sagittal planes of the thoracic limb

Bone	Plane	Joint orientation angle	Acronym
Humerus	Frontal	Mechanical lateral distal humeral angle	mLDHA
Humerus	Sagittal	Mechanical caudal proximal humeral angle	mCdPHA
Humerus	Sagittal	Mechanical cranial distal humeral angle	mCrDHA
Radius	Sagittal	Anatomic cranial proximal radial angle	aCrPRA
Radius	Sagittal	Anatomic caudal distal radial angle	aCdDRA
Radius	Frontal	Anatomic medial proximal radial angle	aMPRA
Radius	Frontal	Anatomic lateral distal radial angle	aLDRA

Table 3

Nomenclature of joint orientation angles measured in the frontal plane of the pelvic limb

Bone	Plane	Joint orientation angle	Acronym
Femur	Frontal	Mechanical lateral proximal femoral angle	mLPFA
Femur	Frontal	Mechanical lateral distal femoral angle	mLDFA
Tibia	Frontal	Mechanical medial proximal tibial angle	mMPTA
Tibia	Frontal	Mechanical medial distal tibial angle	mMDTA

Table 4

Joint orientation angle values for the normal cat and disproportionate dwarfism cat thoracic limb

	Normal cat (*n* = 24) Mean ± SD	**Normal cat (*n* = 24) 95% CI**	**FDD cat (*n* = 10) Mean ± SD**	**FDD cat (*n* = 10) 95% CI**	***p*-Value**
mCdPHA	73.0 ± 3.0	71.8–74.3	46.2 ± 9.1	39.7–52.7	<0.001
mCrDHA	76.7 ± 2.4	75.7–77.7	82.5 ± 7.6	77.0–87.9	0.041
mLDHA	87.9 ± 2.1	87.1–88.9	84.3 ± 5.8	80.1–88.5	0.08
aMPRA	82.7 ± 2.9	81.4–84	75.1 ± 6.0	70.1–80.2	0.009
aLDRA	93.1 ± 2.8	91.9–94.2	82.3 ± 7.1	77.2–87.4	<0.001
aCrPRA	76.9 ± 2.1	76.0–77.8	62.9 ± 8.6	56.8–69.1	<0.001
aCdDRA	76.2 ± 2.5	75.1–77.3	86.9 ± 6.2	82.5–91.3	<0.001

Abbreviations: aCdDRA, anatomic caudal distal radial angle; aCrPRA = anatomic cranial proximal radial angle; aLDRA, anatomic lateral distal radial angle; aMPRA, anatomic medial proximal radial angle; CI, confidence interval; FDD, feline disproportionate dwarfism; mCdPHA, mechanical caudal proximal humeral angle; mCrDHA, mechanical cranial distal humeral angle; mLDHA, mechanical lateral distal humeral angle; SD, standard deviation.

Table 5

Joint orientation angle values for the normal cat and disproportionate dwarfism cat pelvic limb

	Normal cat[18] (*n* = 100) Mean ± SD	**Normal cat (*n* = 100) 95% CI**	**FDD cat (*n* = 10) Mean ±SD**	**FDD cat (*n* = 10) 95% CI**	***p*-Value**
mLPFA	100.5 ± 3.7	99.8–101.2	106.3 ± 3.6	103.7–108.8	<0.001
mLDFA	97.2 ± 2.2	96.7–97.6	103.5 ± 6.2	99.3–108.1	0.009
mMPTA	88.0 ± 3.2	87.3–88.6	97.4 ± 3.3	95.0–99.7	<0.001
mMDTA	107.6 ± 4.8	106.6–108.5	96.1 ± 1.8	94.9–97.5	<0.001

Abbreviations: CI, confidence interval; FDD, feline disproportionate dwarfism; mLDFA, mechanical lateral distal femoral angle; mLPFA, mechanical lateral proximal femoral angle; mMDTA, mechanical medial distal tibial angle; mMPTA, mechanical medial proximal tibial angle; SD, standard deviation.